Macromolecules
PERSPECTIVE

Macromolecules **2009**, *42*, 7605–7615 **7605**
DOI: 10.1021/ma900821k

Large-Strain Mechanical Behavior of Model Block Copolymer Adhesives

Costantino Creton,* Guangjun Hu, and Fanny Deplace†

Laboratoire de Physico-Chimie des Polymères et Milieux Dispersés, CNRS-ESPCI ParisTech-UPMC, 10 rue Vauquelin, 75231 Paris Cedex 05, France. †*Current address: Department of Materials Science and Engineering, University of California Santa Barbara, Santa Barbara, CA 93106.*

Leslie Morgret and Kenneth R. Shull*

Department of Materials Science and Engineering, Northwestern University, 2220 Campus Dr., Evanston, Illinois 60208-3108

Received April 15, 2009; Revised Manuscript Received September 9, 2009

ABSTRACT: Pressure-sensitive adhesives represent one of the most important commercial applications of block copolymers. The large-strain tensile properties of these soft adhesive materials play a dominant role in determining their adhesive properties. In many cases changes in the polymer architecture significantly affect the large-strain properties and the resultant adhesive performance, with little or no effect on the linear viscoelastic properties. In this Perspective we provide several examples, using model systems based on diblock, triblock, tetrablock, and star-block copolymers of polystyrene and polyisoprene.

Introduction

Pressure-sensitive adhesives (PSAs) consist of a thin viscoelastic layer (typically 20−100 μm) with a modulus at the experimentally relevant frequencies in the range of 10^4-10^5 Pa. They find widespread applications in the labeling and packaging industry of course but also as assembling tools when precise positioning and instant adhesion are required. PSAs are a special class of soft materials that stick to nearly any surface upon simple contact.[1] They must have a low elastic modulus and be very dissipative in the viscous sense (the property of a liquid) to stick by simple contact, even to a rough surface, but must also be resistant to creep (the property of a solid), to avoid slow failure under load. Physically or chemically cross-linked polymers above their glass transition temperature (T_g) are the only known types of material that offer this combination of properties which result from having a loose but sufficiently connected network of chains.

Starting from the pioneering work of Kaelble, it was recognized that the viscoelastic properties of PSAs were a key ingredient controlling the application performance. For reasons of experimental convenience the early work focused only on viscoelasticity in the linear (low-strain) regime,[2−8] which provides steady-state properties such as the complex modulus as a function of frequency. Dahlquist proposed that the elastic component of the modulus needed to be below a certain value to form a good contact with a rough surface and that a relatively high value of the loss factor (tan(δ) between 0.3 and 0.5) was needed to provide resistance to detachment.[9] These properties were easily achieved with a sparsely physically or chemically cross-linked polymer network made with a polymer with a low glass transition temperature (around 50−70 °C below the usage temperature).[10] Such sparsely cross-linked networks are commonly produced from natural rubber, diluted with a small miscible molecule or with acrylic copolymers. Both of these systems are still used extensively in pressure-sensitive adhesive formulations.

*To whom correspondence can be addressed. E-mail: k-shull@northwestern.edu,

Beginning in the 1970s, it was realized that properly designed microphase-separated block copolymers could be used to make PSAs.[3,11] These soft networks have exceptional resistance to creep while providing a high level of adhesion. The fact that the PSA films could be processed without using any solvent, by simply heating the block copolymer over the order−disorder temperature (ODT), greatly favored their development in industrial applications.[12]

The mechanisms of adhesion of PSA layers have been elucidated in detail through a series of insightful mechanical experiments, beginning with the work of Zosel in the late 1980s and early 1990s.[10,13,14] These experiments demonstrated that the stickiness or "tack" of the PSA was due to the formation of an optically visible fibrillar structure bridging the adhesive and the adherend during debonding. Zosel identified the crucial role played by the average molecular weight between entanglements in the formation of this fibrillar structure, showing that when the density of entanglements was too high, the fibrils could not form. These conclusions were based on a contact test where a flat-ended cylindrical probe is brought into contact with an adhesive layer and detached under controlled conditions. Using an adhesive film thickness much smaller than the diameter of the cylindrical probe, Zosel clearly demonstrated the load bearing nature of the PSA fibrils. Further experimental advances have led to the identification of the mechanisms by which the fibrils are formed and led to a rather detailed description of the deformation of the adhesive layer.[13,14]

These studies have clearly demonstrated that PSA performance is determined by an interplay between adhesive/substrate interactions and the bulk mechanical properties of the adhesive material.[1] The role of the interfacial interactions is to support a stress that is sufficiently large so that the bulk of the adhesive material can be deformed to the large strains experienced by the adhesive fibrils. Optimization of a PSA therefore requires that two separate materials questions be addressed:

- What controls the stress that the interface can support?
- What controls the large-strain deformation behavior of the adhesive material?

Published on Web 09/28/2009

Costantino Creton is currently C.N.R.S directeur de recherche at the Ecole Supérieure de Physique et Chimie Industrielles (ESPCI ParisTech) in France. He obtained an engineering degree in Materials Science from the Ecole Polytechnique Fédérale de Lausanne (Switzerland) in 1985 and his M.S. and Ph.D. in Materials Science and Engineering at Cornell University in 1991 under the supervision of Professor Edward J. Kramer. After a one year postdoc at the IBM Almaden Research Center in San Jose, he joined the ESPCI in Paris first as a postdoctoral associate in 1993 and, since 1994, as a C.NRS permanent researcher. His research interests include mechanical properties of polymers at interfaces, adhesion of polymers, and deformation and fracture of soft polymer networks. He has received the Polymer Prize from the French Polymer Group in 2002, the Prix Dédale of the French Adhesion Society in 2007, and the Journal of Polymer Science Polymer Physics award in 2008.

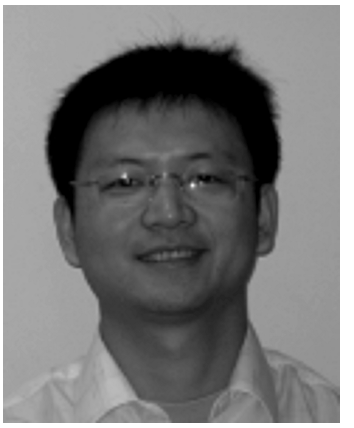

Guangjun Hu received his B.Eng. (with Prof. Liqun Zhang) in Polymer Engineering and Science from Beijing University of Chemical Technology, China. He earned his Ph.D. in Polymer Chemistry and Physics with Prof. Mingshu Yang at Institute of Chemistry, Chinese Academy of Sciences, China. He is presently a postdoctoral fellow with Prof. Costantino Creton at the Laboratoire de Physico-Chimie Structurale et Macromoléculaire of ESPCI/UPMC/CNRS. His postdoctoral research focuses on the mechanical properties of hybrid materials and soft materials.

Fanny Deplace graduated in Physics and Chemistry of Polymers from the Ecole Europeenne de Chimie Polymeres et Materiaux of Strasbourg (France) in 2003. She then moved to Paris and received her M.Sc. (2004) and Ph.D. (2008) in Physics and Chemistry of Materials from ESPCI (with Prof. Costantino Creton). Her dissertation research involved the investigation of the relationship between the nanostructure and the deformation and adhesive properties of waterborne nanostructured acrylic adhesives made of structured core−shell latex particles. She is currently a postdoctoral researcher with Prof. Edward J. Kramer and Prof. Glenn H. Fredrickson at the University of California, Santa Barbara, at the Materials Research Laboratory. Her current postdoctoral research focuses on the processing−structure−mechanical property relationships of semicrystalline polyolefin-based block copolymers and involves the use of small-angle X-ray scattering and wide-angle X-ray scattering to determine the morphological and structural changes of the crystals which occur as the material is subjected to step cyclic tensile processing.

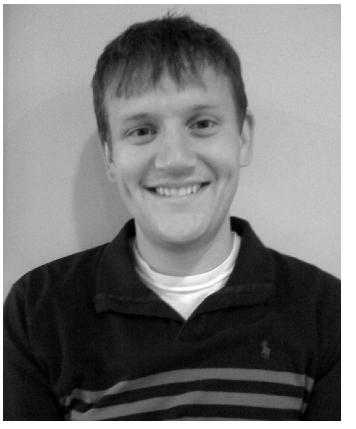

Leslie Morgret recently earned a Ph.D. in Materials Science and Engineering at Northwestern University. He earned his B.S. in Chemical Engineering and minored in Biochemistry at the University of Colorado at Boulder. During his undergraduate career he completed two summer internship programs as NASA Langley Research Center where his research was conducted under the guidance of Dr. Jeffrey Hinkley. His research focused on the synthesis and characterization of thermally responsive poly(*N*-vinylcaprolactam) hydrogels and process optimization of fiber-spun poly(vinylidene fluoride) and poly(ether imide) polymer mats. He began his doctoral program in Material Science and Engineering at Northwestern University in 2004 under the guidance of Prof. Gregory Olson. His doctoral research focused on the design of molecular architectures for the stabilization of large-strain biaxial flow in both model and practical complex polymer systems. In this research he utilized a computational materials design approach for the optimization of processing−structure−property relationships governing large-strain biaxial flow stabilization in complex polymer composites.

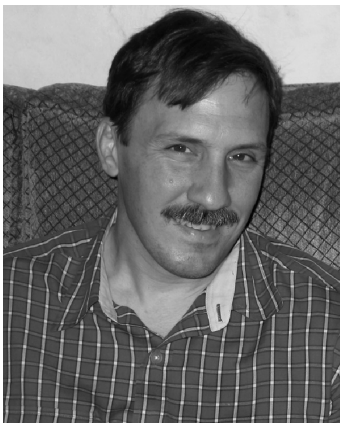

Kenneth R. Shull is Professor of Materials Science and Engineering at Northwestern University, where he is also currently serving as the associate department chair. His research interests involve the interfacial properties of amorphous polymers, with a particular emphasis on adhesion. Recent interests include the large-strain deformation and fracture behavior of "soft" materials including polymer gels and the interfacial behavior of biopolymers. He received B.S. and M.S. degrees in Materials Science from MIT, followed by a Ph.D. in Materials Science from Cornell University, which he received in 1990. He worked as a research staff member at the IBM Almaden Research Center for 3 years before joining Northwestern in 1993. He is a fellow of the American Physical Society and of the Adhesion Society and is also active in the American Chemical Society, Materials Research Society, and the Adhesion Society.

These questions are equally important in the overall design of a soft adhesive. The first question is important in the design of release coatings for PSAs, for example. These coatings must be designed so that stress required to remove the PSA from the backing is less than the stress required to substantially deform the bulk of the material.[15] This Perspective, however, is concerned primarily with the second question because this is the issue where block copolymers have played the greatest role.

Given the obvious importance of the large-strain tensile behavior of the materials in determining the adhesive performance, it is useful to understand how this behavior is affected by the underlying material structure. Block copolymers, used widely as the basis for commercial PSAs as mentioned above, are ideally suited for these types of fundamental investigations. In this Perspective we begin with some general background on the mechanical properties of the types of block copolymers that are of particular relevance in soft adhesive applications. We then discuss results for the mechanical response of styrenic block copolymers and conclude with some adhesive characterization of these styrenic materials.

Background

Nonlinear Elasticity and the Neo-Hookean Limit. While the thermodynamics of microphase-separated structures of block copolymers and their blends has been extensively investigated,[16] the mechanical properties of pure block copolymers have been comparatively less studied, in particular because mechanical testing requires a larger amount of material that is widely available only for selected microstructures and chemistries.[17−19] When mechanical properties are concerned, the nature (glassy or rubbery) and the type of organization (lamellae, cylinders, gyroid, spheres) of the immiscible blocks have a profound effect on the macroscopic mechanical behavior.

Because of the expected interesting anisotropic properties, many published investigations have focused on the situation

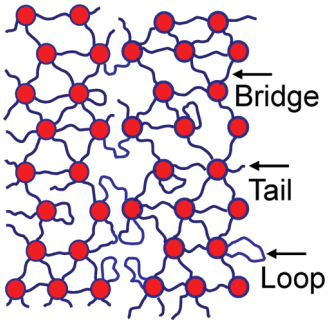

Figure 1. Schematic structure of an elastic block copolymer network, showing bridging and looping configurations of triblock copolymer midblocks and tails originating from the addition of diblock copolymer. The spheres represent the glassy end block domains.

where the block copolymer self-organizes over a long distance in a lamellar or a cylindrical structure.[22−25] These structures are of limited use for adhesive applications and will not be considered in detail here. We will instead focus on another very interesting feature of ordered block copolymer structures, namely their ability to introduce a dilute but highly regular density of cross-link points. This type of ordered structure can be obtained when the volume fraction of the minority phase is less than 15%, and the block copolymers self-assemble in a structure of spheres in a matrix, as illustrated schematically in Figure 1. From the point of view of mechanical properties and adhesive applications, the most common type of material is an A−B−A triblock copolymer where the A block is glassy and the B block is elastomeric. This results in an elastomeric material which is very similar to a chemically cross-linked rubber at room temperature but becomes a low-viscosity polymeric fluid above the order−disorder temperature. Such a material is commonly called a thermoplastic elastomer. The mechanical properties of some of the commercially produced grades of styrene−isoprene or styrene−butadiene were extensively characterized in the 1960s and 1970s as potential substitutes for rubbers. This first generation of materials was mostly comprised of triblock copolymers and may have contained poorly controlled amounts of diblock copolymers.

While relatively few systematic investigations of the effect of the architecture of the block copolymers on the large-strain mechanical properties have been carried out, progress has certainly been made in the ability to place these properties in the general context of rubber elasticity theory. The starting point for these models is usually the strain energy density function for a neo-Hookean material, which has the following form:[17]

$$U^n = \frac{E}{6} J_1; \quad J_1 = \lambda_1^2 + \lambda_2^2 + \lambda_3^2 - 3 \tag{1}$$

Here U^n is the strain energy per unit volume for this neo-Hookean reference system, E is Young's modulus, λ_1, λ_2, and λ_3 are the principal extension ratios, and $J_1 + 3$ appearing in eq 1 is the first strain invariant as usually defined in solid mechanics. The small compressibility of these materials can generally be ignored, so that the shear modulus is given by $E/3$ and $\lambda_1\lambda_2\lambda_3 = 1$. A consequence of this assumption of incompressibility is that the elastic properties in the linear regime are completely specified by a single parameter. While there is no compelling reason to use E as opposed to the shear modulus, we use E in this Perspective because we have historically been interested in the testing

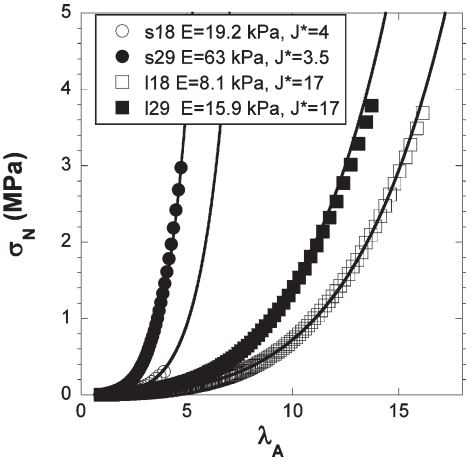

Figure 2. Stress–strain behavior for an unentangled block copolymer gel. The solid lines are fits to eqs 4 and 5, using the indicated values for E and J^*.

of soft adhesive materials in an extensional geometry where it is sensible to express the results in terms of Young's modulus.

The specific value of E depends on the cross-linking conditions. If the material deforms affinely, and the network strands between cross-link points are described by Gaussian statistics, then E is given by the concentration of elastically effective network strands, ν_e:

$$E = 3\nu_e k_B T \tag{2}$$

For triblock copolymers in the limit where entanglements do not play a role, ν_e is simply given by the inverse of the molecular volume, v_p, multiplied by f_b, the fraction of triblock copolymers with "bridging" midblocks that span different end block domains. For the block copolymer systems of interest here, this simple picture is complicated by the finite size of the end block domains and by the distortion of the midblock chains from their ideal Gaussian configurations. These are relatively small corrections, typically a factor of 2 or less, and do not substantially affect the most relevant qualitative features of mechanical response. More important effects include the finite extensibility of the midblocks, responsible for strain hardening of these materials, and the role of physical entanglements that have a more pronounced effect on the mechanical response at low strains than at large strains. These effects are discussed in general terms in the following section.

Strain Hardening in Unentangled Triblock Copolymer Gels. Equation 1 is valid for relatively low strains, where the bridging midblocks in the triblock copolymer structure can be viewed as linear springs. This approximation breaks down at sufficiently large strains, where the separation between domains approaches the contour length of the midblock itself. Various modifications to the strain energy function have been proposed to account for this effect, including a simple form suggested by Gent that diverges when J_1 reaches some critical value.[18] The following form has a similar behavior, but without a divergent stress field for finite J_1, an important factor when using this strain energy function in finite element simulations.[19]

$$U^e = \frac{EJ^*}{6}(\exp(J_1/J^*) - 1) \tag{3}$$

Here U^e is the elastic strain energy for this exponential strain-hardening model, and J^* is a characteristic value of J_1 above

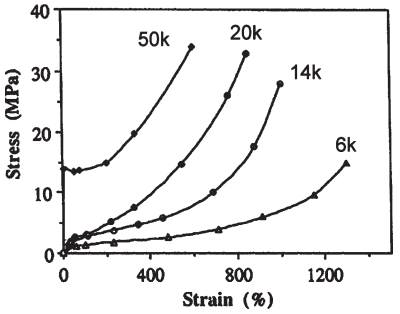

Figure 3. Stress–strain curves for PMMA–PBD–PMMA triblock copolymers. Each of the midblocks has a molecular weight of 80K, and the molecular weights of the PMMA end blocks are indicated in the plot (from ref 22).

which strain hardening effects dominate the material behavior. Equation 3 is convenient because the strain hardening is described by a single parameter, J^*, and the neo-Hookean form (eq 1) is recovered at small strains or alternatively for $J^* \to \infty$. Also, the model predicts an exponential increase in the stress for any applied deformation. We are specifically interested in uniaxial extension ($\lambda_1 > 1$) and compression ($\lambda_1 < 1$), both of which have $\lambda_2 = \lambda_3$. For the compression data we generally use the area extension ratio, λ_A, as the measure of strain, with $\lambda_A = \lambda_2\lambda_3 = 1/\lambda_1$. The nominal stress (force divided by undeformed cross section) in this case is given by the following expression:

$$\sigma_N^e = \frac{\partial U^e}{\partial \lambda_1} = \sigma_N^n \exp(J_1/J^*) \tag{4}$$

where $J_1 = \lambda_1^2 + 2/\lambda_1 - 3$ and σ_N^n is the nominal stress obtained for a neo-Hookean material:

$$\sigma_N^n = \frac{E}{3}(\lambda_1 - 1/\lambda_1^2) \tag{5}$$

For the data shown in this Perspective we drop the subscripts and define λ as λ_1 in a uniaxial extension experiment.

Triblock copolymer gels are excellent systems for investigating the importance of strain hardening in the absence of additional complications originating from entanglements. Thermoreversible gels are particularly useful because the network structure forms at solution concentrations that are low enough so that entanglements between midblock polymers are eliminated, a result that is evident from the following relationship between the entanglement molecular weight, M_e, and the polymer volume fraction, ϕ_p, for polymer solutions:[20,21]

$$M_e = M_e^0 \phi_p^{-4/3} \tag{6}$$

where M_e^0 is the entanglement molecular weight for the undiluted polymer. Figure 2 shows data for acrylic triblock copolymer gels for which the midblock molecular weights are below M_e, so that entanglement effects do not need to be taken into account.[19] The exponential hardening predicted by eq 4 is observed, with values of J^* that are consistent with the maximum extensibility of the copolymer midblocks.

General Behavior of Triblock Copolymer Melts. Entanglements play a dominant role in the behavior of both thermoplastic elastomers and pressure-sensitive adhesives that are based on multiblock copolymers. The role of entanglements in the context of the strength of thermoplastic elastomers has

Table 1. Molecular Characteristics of the Styrene (S)−Isoprene (I) Copolymers Used in the Experiments[a]

	S mol wt (kg/mol)	I mol wt (kg/mol)	S mol wt (kg/mol)	I mol wt (kg/mol)	wt % S	wt % bridgeable isoprene
SI diblock	10.8	61			15	0
SIS-a triblock[b]	11.6	131	11.6		15	100
SIS-b triblock[b]	10.6	97	10.6		18	100
SISI tetrablock	12.4	60	12.4	70	16	46
$(SI)_4$ 4-arm star block	10.8	61			15	100

[a] The star block can be viewed as four diblock copolymers with the molecular weights indicated in the table, joined together at the polyisoprene ends. [b] SIS-b was used to generate the data shown in Figures 7, 11, and 12. SIS-a is the triblock copolymer used in all other experiments.

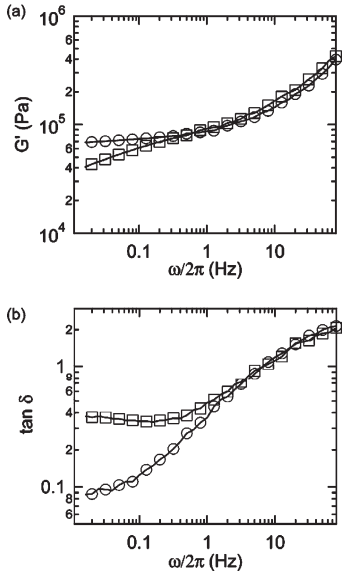

Figure 4. Storage modulus G' (a) and loss tangent tan(δ) (b) as a function of frequency at $T = 22$ °C, for SIS-a/SI blends with 60 wt % resin: (○) 0 wt % SI; (□) 54 wt % SI.

been demonstrated by the synthesis and characterization of an excellent set of model systems by the Jerôme group.[22−28] One of the conclusions that has emerged from this work is that the ultimate tensile strength of pure triblock copolymers increases when the entanglement molecular weight of the soft, rubbery midblock is decreased.[25] Triblock copolymers with poly(methyl methacyrate) end blocks and a polybutadience midblock ($M_e^0 \approx 1700$ g/mol) have a higher tensile strength than the corresponding triblock copolymers with poly(*n*-butyl acrylate) midblocks ($M_e^0 \approx 28\,000$ g/mol). We attribute this result to the strain softening that is observed in entangled systems, which leads to a redistribution of stresses to a larger volume in the vicinity of a propagating crack, thereby increasing the energy dissipation associated with crack propagation and increasing the toughness. This effect plays an important role in the behavior of pressure-sensitive adhesives and is discussed in more detail below.

The elastomeric character of block copolymer melts generally requires that the overall volume fraction corresponding to the hard blocks be less than about 15%. At higher volume fractions the glassy phase exists as a continuous network of rigid cylinders or lamellae, stiffening the material and giving a yield point at relatively low strains. The effect is illustrated in Figure 3, which shows stress−strain curves in uniaxial extension for PMMA−PB−PMMA triblock copolymers with a constant midblock length and increasing end block lengths.[22] This figure is an excellent illustration of the dramatic changes in mechanical properties that accompany changes in the domain morphology from glassy spheres (6K end blocks) to glassy cylinders (14K and 20K end blocks) to lamellae (50K end blocks).

Model Styrenic Systems

While the examples from the previous section illustrate the existence of mechanical data for a range of chemical compositions, perhaps the most carefully characterized and commercially useful system is the case where the end blocks are polystyrene, and the midblock is *cis*-1,4-polyisoprene. For pressure-sensitive adhesive applications a triblock copolymer is often blended with diblock copolymer (either intentionally or as a consequence of the polymerization reaction), thereby reducing the midblock bridging fraction and decreasing the tensile strength of the material. In addition, these diblock/tribock blends are often further diluted with a high T_g, low molecular weight molecule that is miscible with the elastomeric domains and immiscible with the glassy domains. These low molecular weight diluents are generally referred to as tackifying resins in the industrial community and are necessary to dilute the entanglement network, lower the elastic modulus, and transform the rubbery and nonadhesive pure block copolymer into a much softer and viscoelastic material that acts as an effective PSA.[7,29] Although the microstructure of the blend is mainly determined by the volume fraction of PS, similar to the behavior illustrated in Figure 3, its mechanical properties are greatly dependent on the architectures of the block copolymers that are being used. It is the purpose of this section to explore the effect of copolymer architecture in more detail.

Diblock/Triblock Blends. The easiest comparison to make is between a pure A−B−A triblock copolymer and a 50/50 blend of a triblock copolymer with an A−B diblock with the same polystyrene content but one-half the total molecular weight. Triblock copolymers with PS end blocks have the ability to bridge adjacent PS domains while diblock copolymers do not. This bridging capability of the midblock does not significantly affect the undeformed morphology but greatly affects the mechanical strength.[30,31] In the rest of this Perspective we will refer to bridging chains and pendant chains for these two situations. For the pure triblock copolymers, mean-field simulations have shown that about 80% of the midblocks act as bridging chains while the rest act as loops.[32,33] This result remains true when the blend is diluted with a tackifying resin to an overall polymer concentration of 40 wt %. If diblocks with one-half the molecular weight of the triblock are added to the blend, the concentration of bridging chains scales linearly with the triblock volume fraction in the diblock/triblock blend.[32] We also discuss results using S−I−S−I tetrablocks, and four-arm star-block copolymers, described in more detail below. The characteristics of each of the copolymers are listed in Table 1. Note that two closely related triblock copolymers, referred to as SIS-a and SIS-b in Table 1, have been used in these experiments.

Figure 4 shows the small strain complex shear modulus measured in a parallel plate rheometer as a function of frequency for SIS material and a SI/SIS blend with 54 wt % SI, relative to the total amount of copolymer. Each material also contains 60 wt % resin. The resin ($T_g = 40$ °C) is a hydrogenated polycyclopentadiene produced by Exxon

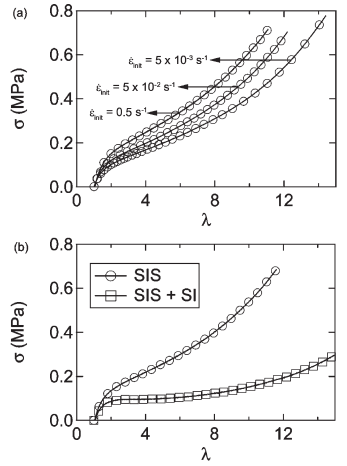

Figure 5. Nominal stress as a function of extension ratio for SIS-a/SI blends with 60 wt % resin: (a) tensile tests for the 0 wt % SI blend at initial strain rates of 5×10^{-3}, 5×10^{-2}, and 0.5 s^{-1}; (b) tensile tests at 0.5 s^{-1} for blends with 0 and 54 wt % SI.

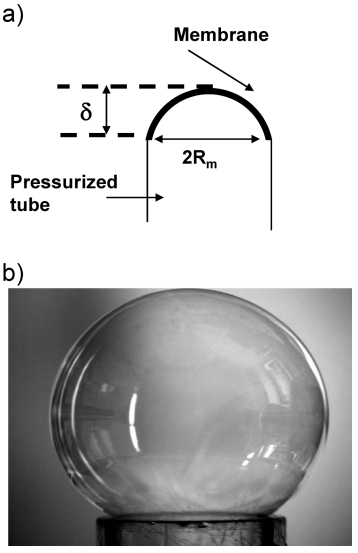

Figure 6. (a) Membrane inflation geometry for biaxial stretching of thin polymer films. (b) Representative image of an inflated membrane.

Mobil Chemical under the trade name of Escorez 5380. The introduction of a diblock copolymer results in a slight decrease in G' at low frequency and increases more significantly the value of the loss tangent. Both effects are only apparent at frequencies lower than about 1 Hz. If tensile tests are performed up to several hundreds of percent strains on the same materials, a relatively weak strain rate dependence is observed (see Figure 5a) for a given blend, and a strong effect of the presence of the diblock on the softening behavior is observed at a given strain rate (see Figure 5b). Because these experiments are conducted with a constant crosshead velocity, V, the actual true strain rate decreases throughout the test. The reported strain rates correspond to the initial strain rates, $\dot{\varepsilon}_{init}$, obtained by dividing the crosshead velocity by the undeformed sample length (i.e., by the sample dimension in the direction of the applied deformation). The primary effect of the presence of the diblock is to modify the shape of the stress−strain curve, giving a more pronounced softening (negative curvature in the stress/strain curve) followed by strain hardening (positive curvature) at higher strains.

Strain softening is also observed in a biaxial extension geometry. These biaxial extension measurements were performed by spin-coating a thin layer of SIS or an SIS/SI blend onto a salt crystal and transferring it to a water bath and then onto an open cylindrical tube. Pressurization of the tube inflates the membrane as shown schematically in Figure 6a. A representative image for a large biaxial extension is shown in Figure 6b. If the overall shape of the inflated membrane can be approximated as a sphere, as is often the case, the average area extension, λ_A, is given by the following expression:[34]

$$\lambda_A = 1+(\delta/R_m)^2 \tag{7}$$

where δ is the vertical extension of the membrane, R_m is the radius of the undeformed membrane, and λ_A is defined as the ratio of the deformed and undeformed membrane areas. A quantitative analysis of the data is complicated by the nonuniform strain state within the inflated membrane[35] but is simplest at the apex where the membrane is in a state of equibiaxial stress. In this region the membrane tension is given by the following expression:

$$T = \frac{PR_0}{2} \tag{8}$$

where R_0 is the radius of curvature at the apex and P is the inflation pressure. The elastic contribution to the membrane tension is obtained by subtracting the contribution from the two free surfaces of the membrane:

$$T_e = T - 2\gamma \tag{9}$$

Strain softening in entangled systems is observed in both uniaxial extension and equibiaxial extension, as illustrated by the data in Figure 7. The uniaxial data in Figure 7a correspond to the measured nominal tensile stresss, normalized by the neo-Hookean values given by eq 5. The data in Figure 7b were normalized by the neo-Hookean elastic tension, T_e^n, given by the following expression:

$$T_e^n = \frac{Eh}{3}\left(1-\frac{1}{\lambda_A{}^3}\right) \tag{10}$$

The relationship between the local area extension at the apex and the average value given by λ_A depends on the detailed constitutive relationship for the rubber. For typical rubbers the area extension in this region exceeds λ_A by a factor of about 2, a correction that we have not used here because we are interested primarily in the qualitative nature of the strain softening.[35] Because of this correction, the values for the elastic moduli shown in Figure 7b should be viewed as upper bounds to the actual values, so that the moduli obtained from the biaxial extension experiments are actually substantially lower than the moduli obtained from the uniaxial extension measurements. We attribute this result to a reduced entanglement density in the spuncast films used in the equibiaxial extension experiments. The phase-separated morphology forms during the casting process while the films exists in a transient, solvent-rich gel state, with an entanglement density that is reduced by the presence of the solvent. As the solvent evaporates, the relaxation time associated with molecular exchange between polystyrene aggregates is too long for the structure of the dried material to equilibrate, so the entanglement density and low-strain

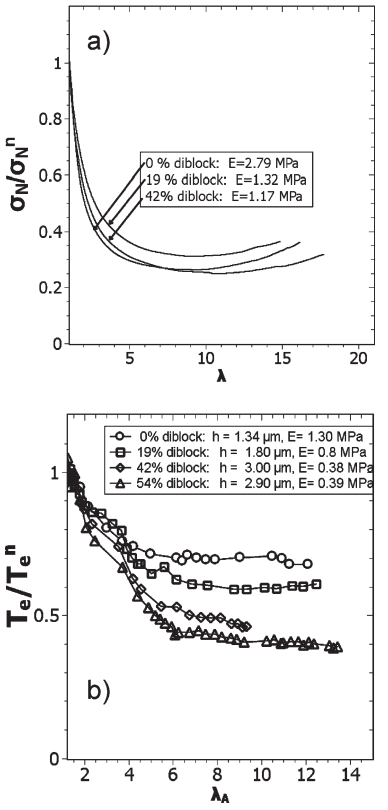

Figure 7. Nominal stress in uniaxial tension (a) and elastic membrane tension in equibiaxial extension (b) for diblock/triblock blends. Stresses and membrane tensions are normalized by the values corresponding to a neo-Hookean material.

elastic modulus remain lower than one would expect for a truly equilibrated film. Similar phenomena have been observed previously in systems where the solvent preferentially dissolves the rubbery midblock of the triblock copolymer.[36,37]

The important qualitative result illustrated by the data in Figure 7 is that strain softening is observed for both uniaxial and equibiaxial extension. From the molecular point of view this result can be interpreted as follows: the small strain modulus is controlled by the density of entanglements which act as cross-link points but progressively slip and orient in the direction of traction.[38] The fractional softening observed in uniaxial extension at intermediate strains is not strongly dependent on the fraction of bridging midblocks, as illustrated by the data in Figure 7a.

Effect of Copolymer Architecture: Triblock/ Diblock Blend vs Tetrablock. A striking example of the role played by the copolymer architecture is provided by the comparison between a diblock/triblock blend and an A−B−A−B tetrablock copolymer. In a recently proposed molecular model of the linear viscoelastic behavior, Gibert et al. reduce the triblock/diblock blends to a blend of bridging chains and pendant chains.[39,40] Their model suggests that a properly designed A−B−A−B tetrablock copolymer could have identical linear viscoelastic properties to a blend of A−B diblock and A−B−A triblock. Three conditions are necessary in order for this equivalence to be achieved: (i) The A content needs to be constant in order to maintain the same thermodynamically stable structure (spheres of A in a matrix of B). (ii) The molecular weight of the B free end-block in the ABAB chains has to be the same as that of the B sequence of diblock chains in the ABA + AB blend. (iii) The length of the B blocks trapped between two A blocks in the ABAB

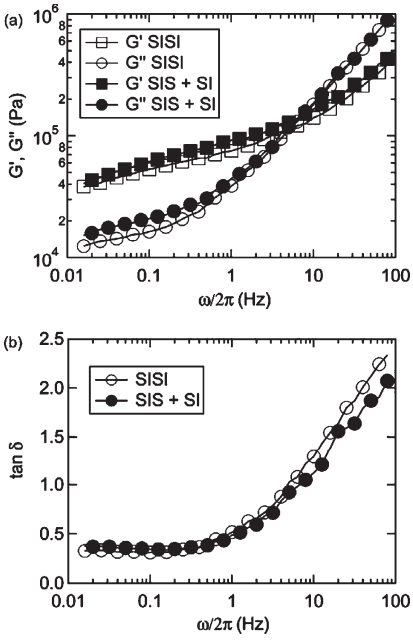

Figure 8. Linear viscoelastic properties for the adhesive blends based on SIS-a + SI with 54% SI and on SISI: (a) G' and G'' and (b) tan δ.

chains has to be chosen in order to respect the same "pendant B chains/bridging B chains" ratio. Therefore, the length of the equivalent triblock in the ABAB chains could not be equal to the length of the triblock chains in ABA + AB blends.

In order to test these ideas, a SISI tetrablock copolymer was synthesized by ExxonMobil Chemical. The polymer had an overall styrene fraction of 16 wt % with 46.2 wt % of the polyisoprene corresponding to the "bridgeable" block between styrene blocks. The molecular weight of the non-bridgeable block is just slightly higher than the polyisoprene block of the SI chains. As expected, the linear viscoelastic properties of a SISI tetrablock and a SIS/SI blend are nearly identical, provided that they are formulated according to the three criteria listed above. Room temperature data for the specific blend used by Roos[41,42] are shown in Figure 8 and confirm the similarity of the linear viscoelastic properties of these materials. Gibert et al. have obtained similar results over a much broader temperature and frequency range, even with the addition of substantial resin fractions.[43]

An important difference between the SISI and tetrablock and the SIS/SI blends is that the tetrablock has a covalent bond linking the equivalent triblock and diblock chains. Therefore, while no difference is seen in the linear viscoelastic response, we would expect to see differences in the large-strain mechanical properties and consequently on their adhesive properties. The expected differences in the large-strain tensile properties are illustrated by the comparison shown in Figure 9. The tensile curves of the tetrablock-based adhesive and the corresponding SIS/SI-based adhesive are extremely different. We also have represented for comparison the pure SIS blend data of Figure 5. In both cases there is a linear increase in the stress at low strains, followed by strain softening and then strain hardening regimes. Reduction in the bridging fraction by the addition of the additional polyisoprene block or by the addition of the SI diblock copolymer increases the strain softening, but the details depend on the way the decrease in bridging fraction is achieved. Use of tetrablock chains causes the hardening to occur at much lower strains (~600% as compared to 1200% for the SIS/SI blend).

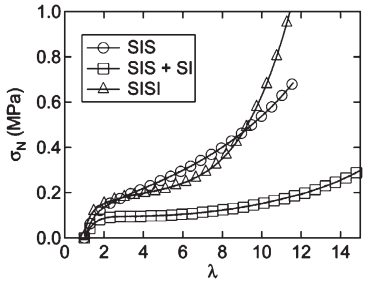

Figure 9. Nominal tensile stress as a function of uniaxial extension for the adhesive blends based on SISI, on SIS-a + SI, and on SIS-a at = $0.5\ s^{-1}$ ($T = 22$ °C). The data are those of Figure 5b with the addition of the SISI data. Resin content for all blends is 60 wt %.

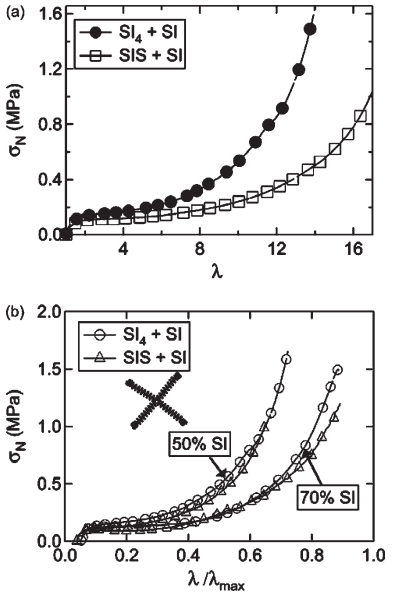

Figure 10. Uniaxial tensile data for the SIS-a/SI and SI4/SI blends for $0.5\ s^{-1}$ and $T = 22$ °C. (a) Nominal stress vs λ for the SI4/SI blends and the SIS-a/SI blends. In both cases the percentage of diblocks in the copolymer blend is 50%. (b) Same data plotted as a function of λ/λ_{max}. The percentages on the figure are the percentages of diblock in the blends. Values of λ_{max} are 19 and 26 respectively for the SI4 and SIS-a.

Although an unambiguous molecular interpretation of these results is difficult to make, the results clearly show that the architecture-dependent connectivity between polystyrene domains can be discerned much more clearly from large-strain measurements and are often difficult to see from measurements of linear viscoelasticity. Given the large strains involved in the debonding processes of soft adhesives, this result implies that it is also difficult to predict quantitatively the adhesive performance from the linear viscoelastic properties.

Effect of Copolymer Architecture: Star vs Linear. Another example of the effect of copolymer architecture is obtained from a comparison involving a four-arm star-block copolymer, $(SI)_4$, which has the branch point at the ends of the polyisoprene blocks of the constituent arms. Each arm of the star corresponds to one SI diblock or to one-half of the SIS triblock. Hence, the total molecular weight of the star is twice that of a triblock. Comparison between a $(SI)_4$/SI blend and a SIS/SI blend (each containing 60% resin) shows two important differences. First, the $(SI)_4$/SI blend softens for higher levels of stress, indicating a higher density of cross-links or trapped entanglements, and the finite extensibility of the SI_4/SI blend is apparent for lower values of λ. The

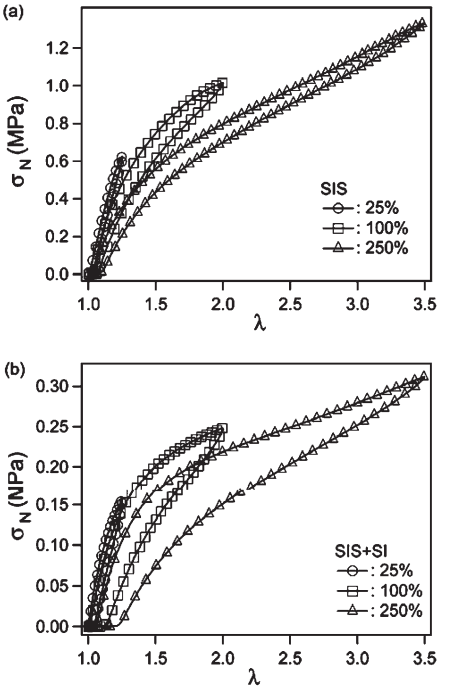

Figure 11. Step-cycle tests for block copolymers materials without resin: SIS-b (a) and a SIS-b/SI blend with 54 wt % SI (b). Percentages indicate the maximum strain experienced for each cycle.

difference in the finite extensibility and in the density of cross-link points is very clear from the tensile tests (see Figure 10a). If we say that the finite extensibility of the blend should scale as the square root of the molecular weight between chemical or physical cross-link points, the star tensile curve should be moved to lower extensions by a factor $\sqrt{2}$, which is the case in Figure 10b. This result is illustrated by renormalizing the deformation by the theoretical maximum extension λ_{max}. On the basis of the value of R_g in the melt,[44] λ_{max} is equal to 19 and 26 respectively for the SI_4 and SIS copolymers.

Large-Strain Hysteresis. Because the adhesion energy is determined by the energy expended in deforming the adhesive material, experiments designed to quantify the mechanical hysteresis are instructive. Figure 11 and Figure 12 show results obtained for blends without resin and with 60 wt % resin at room temperature. On each graph we show results for successive tensile tests carried out on the same sample, with values of the maximum extension, λ_{max}, increasing from 1.25 to 2 to 3.5. A hysteresis loop was considered complete when a sample was stretched to each λ_{max} at a ramp of 5 mm/min, corresponding to an initial strain rate of $0.005\ s^{-1}$, and then came back to zero force. The extension was recorded by a laser video-extensometer following the distance between two marks in the middle part of the stretched sample. There was a 120 s break between each hysteresis loop to release the residual stress. The hysteresis loops for increasing values of the maximum extension, λ_{max}, are plotted for each material. The area in the center of a hysteresis loop is a direct representation of the dissipated energy.

The pure SIS material displays little hysteresis with or without added resin. The only difference being the initial modulus E which drops from approximately 3 to 0.4 MPa as resin is added, consistent with rheological data. The situation is very different when 54% of diblock copolymer is present. The hysteresis becomes much larger, in particular for extensions above 2. Furthermore, the added resin plays a

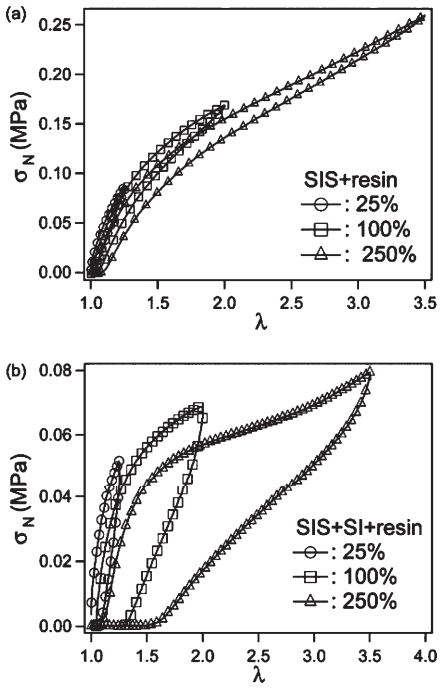

Figure 12. Step-cycle tests for block copolymers blends with 60 wt % resin: SIS-b (a) and SIS-b/SI blend with 54 wt % SI (b). Percentages indicate the maximum strain experienced for each cycle.

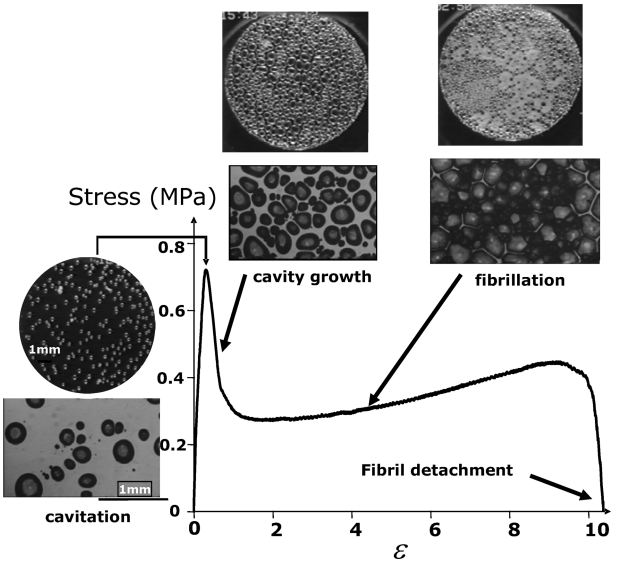

Figure 13. Debonding of an SIS-a/SI PSA blend from a steel surface. The blend consists of 60% resin, and 42% of the block copolymer is SI diblock. The stress represents the force normalized by the initial area of contact, and the strain is the displacement of the probe normalized by the initial thickness of the PSA film.

significant role in increasing the hysteresis at high strains. This is exactly the deformation range found at the edge of a debonding front of an adhesive. Indeed, the material containing 54% of adhesive is much stickier than the pure SIS, while maintaining a similar initial modulus due to the entanglement structure.

While the experimental protocol used in these experiments is similar to the standard tests used to detect the Mullins effect in filled elastomers,[45] no real Mullins effect was identified in our materials. Indeed, the energy dissipation we measured does not seem to be due to the breakage of an organized structure but more to classic viscoelastic dissipation at the macromolecular scale. It is interesting however to note that while the resin substantially increases the glass transition temperature and the monomer friction coefficient at room temperature,[7] it does not greatly affect the shape of the loading curves. On the other hand, the unloading curves for the SIS + SI blend are significantly affected by the presence of this high-T_g resin, implying a slowing down of the relaxation of the stretched polymer chains.

Overall, we observe that, within this range of molecular weights that are much larger than the average molecular weight between entanglements, the molecular weight of the midblock has an important effect on the maximum extensibility and on the softening at intermediate strains, but it has no discernible effect on the linear viscoelastic properties. On the other hand, the ratio of pendant chains to bridging chains has a very important effect on the dissipative properties on the blend, in addition to its effect on the large-strain properties.

Adhesive Behavior. As mentioned in the Introduction, block copolymer blends of the sort described in this Perspective find interesting applications as pressure-sensitive adhesives. An important requirement of a good PSA is that interfacial bond failure by crack propagation be limited, even when the adhesive forces are due to relatively weak van der Waals forces. The material must also maintain a distinctly solid character, exhibiting minimal creep under a constant low level of stress. The capability to resist interfacial crack propagation is typically tested by bringing a flat ended or spherical probe in contact with the adhesive film and subsequently removing it at a constant velocity.[10,14] An example of such a debonding curve for a flat-ended probe removed from a 100 μm thick layer of SIS/SI adhesive blend with 42% diblock is shown in Figure 13.[41] These data are plotted as a function of the engineering strain, ε, with $\varepsilon = \lambda - 1$. The force−displacement curve extends with a nonzero force up to distances several times the initial thickness of the film. The images taken during the debonding process show that the first initial peak is due to the nucleation of a series of cavities, with a size comparable to the thickness of the film, and the subsequent plateau is due to the extension of a fibrillar foam in the direction of traction until the fibrils detach cleanly from the surface. The formation of a such a highly extended foam is a clear signature of the high resistance to interfacial crack propagation of the adhesive/substrate interface. This general scenario occurs for all the styrene/isoprene block copolymer blends discussed here. However, the detailed shape of the force displacement curve varies.[41,46]

Typical debonding curves are shown in Figure 14 for the different SI block copolymer blends discussed above. The level of the plateau in stress during the extension of the fibrillar foam is clearly related to the large-strain tensile test as can be readily seen by comparing Figure 14a with Figure 5b (SIS/SI blends), Figure 14b with Figure 9 (SIS/SI blend and SISI tetrablock), and Figure 14c with Figure 10 (SI_4/SI and SIS/SI blends). It is particularly noteworthy to see that while the small strain moduli of the SIS/SI, SISI, and SI_4/SI materials are all very similar at the typical strain rate applied during these probe tests, the level of stress required to extend the fibrillar foam varies significantly with the copolymer architecture. Such differences in the resistance to fibril extension during debonding lead to important differences in the adhesive properties evaluated by industry-standard methods.[43,47]

Finally, Figures 11 and 12 show that at low strain rates and at intermediate strains the presence of pendant chains increases the level of dissipated energy during stretching of the

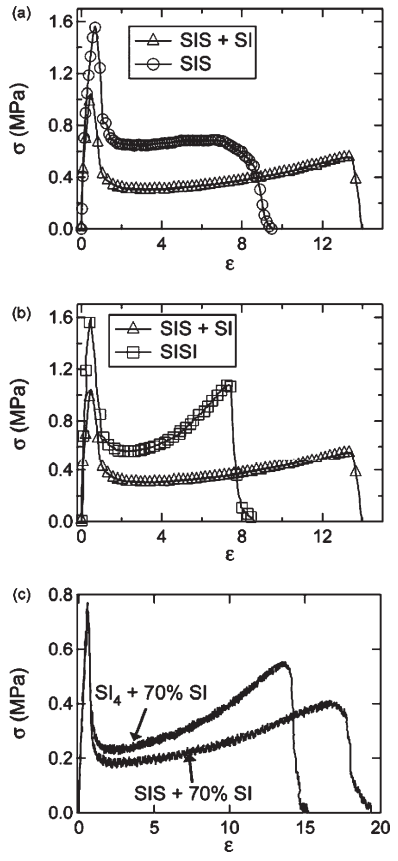

Figure 14. Tensile part of the nominal stress vs strain curves obtained on 100 μm thick layers of PSA with a cylindrical flat−ended steel probe. (a) Comparison of the SIS-a and SIS-a/SI blend with 54% SI (V = 100 μm/s). (b) Comparison of the SIS-aI tetrablock and the SIS-a/SI blend with 54% SI (V = 100 μm/s). (c) Comparison of the SI4 and SIS-a/SI blend with 64% SI (V = 10 μm/s). Each material contains 60% resin.

material. This different level of hysteresis has an important effect on the adhesive properties. These differences become increasingly obvious when the adhesive blends are detached from surfaces where van der Waals forces are weaker, such as a polyolefin surface.[48] In this case the stress−strain curve and the resulting foam structure formed during the debonding of the adhesive layer depend markedly on the competition between the interfacial crack propagation process and the extension of the walls of the foam in the tensile direction. The development of an appropriate adhesive failure criterion, integrating both interfacial interactions and topography and the rheological properties of the adhesive, remains an important unsolved problem for these highly dissipative materials. The difficulty arises from the need to couple the highly nonlinear, large-strain mechanical behavior of the material with an accurate description of the boundary conditions.

In spite of these difficulties, some important progress has been made in describing the micromechanics of adhesive failure in highly deformable elastics solids. The initial stages of the debonding (cavitation vs interfacial crack propagation) have been analyzed for elastic layers[49] and more recently for viscoelastic layers.[50,51] The late stages of the debonding process (fibril formation and detachment) have bee described with solid mechanics models.[52,53] A full-fledged mechanistic model has also been developed to describe the complete debonding of perfectly bonded viscoelastic fluid layers.[54,55] These micromechanical models illustrate the important role played

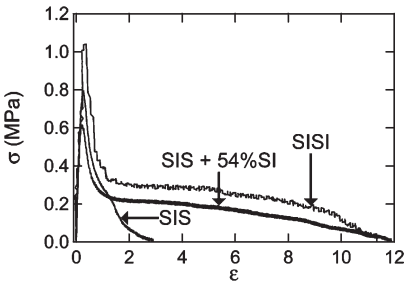

Figure 15. Tensile part of the nominal stress vs strain curves obtained on 100 μm thick layers of PSA with a cylindrical flat-ended EP coated probe. Comparison between the SIS-a and SIS-a/SI blends with the SISI tetrablock (V = 10 μm/s). Each material contains 60% resin.

by the following features: (i) Viscoelastic dissipation at the edge of the moving crack, which retards crack propagation. (ii) Strain softening behavior of the material at intermediate strains, which controls the nature of the "blunted" crack tip at the periphery of a debonded zone. Strain softening acts to reduce the mechanical driving force for adhesive failure at intermediate strains. (iii) Strain hardening at large strains, which controls fibril stability and fibril detachment.

An example of the effect of block copolymer architecture on the 3D debonding structure is shown in Figure 15, where the three adhesive blends are debonded from an ethylene−propylene (EP) surface. The increased hysteresis and marked strain softening brought by the presence of the pendant chains of the diblock copolymer and of the SISI strongly tilts the balance toward fibril formation and prevents the interfacial crack propagation which is observed for the SIS based adhesive. Note also that the combination of the more pronounced strain hardening at large strains of the SISI combined with the softening at intermediate strains due to the presence of the pendant chains results in a higher tensile stress and a fibrillar structure.

This very marked strain softening and large-strain hysteresis, while maintaining a clearly solid and nonflowing character at small strains, is a significant advantage of the block copolymer systems for the adhesive applications. Simple sparsely cross-linked networks made by free radical polymerization of acrylic copolymers can only be made viscoelastic by introducing a significant amount of network imperfections which in turn negatively affect creep resistance.

Conclusions

The focus of this article has been on the relationships between the molecular architecture of block copolymers and block copolymer blends, the large-strain behavior of these materials, and their adhesive performance. Examples have been provided to highlight the importance of factors affecting the large-strain response and the related tack behavior but that have little or no effect on the linear viscoelastic properties. Specific examples for spherical domain morphologies, with spherical glassy domains in a rubber matrix, are as follows:

- Reducing the bridging fraction by the addition of diblock copolymer substantially enhances the observed strain softening and delays the onset of strain hardening to much larger strains (Figure 5b).
- Entanglements contribute to the modulus at low stresses, but the effect of entanglements diminishes at higher stresses, resulting in a substantial strain

softening of the material relative to the prediction for a neo-Hookean material.
- Energy dissipation is increased substantially by a reduction in the fraction of bridging chains between glassy domains (Figures 11 and 12).
- The stress/strain curves measured during a tack curve (deformation of a thin film along its thickness direction by adhesive contact with an indenter) mimic the results obtained from standard tensile tests (comparison of Figure 14 with Figures 5, 9, and 10). Correlation of adhesive performance to large-strain mechanical response is much stronger than the correlation to linear viscoelastic properties.

Acknowledgment. C.C. gratefully acknowledges the financial support of the European Commission under the GROWTH program of the fifth framework program (Project No. G5RD-CT2000-00202 DEFSAM) as well as the collaboration with Jacques Lechat, Nicolas Kappes, and Ken Lewtas from ExxonMobilChemical Europe within the framework of this project. K.S. acknowledges funding from the National Science Foundation, Division of Material Research.

References and Notes

(1) Creton, C. *MRS Bull*. **2003**, *28*, 434.
(2) Kaelble, D. H. *J. Macromol. Sci., Rev. Macromol. Chem. Phys.* **1971**, *C6*, 85.
(3) Kraus, G.; Jones, F. B.; Marrs, O. L.; Rollmann, K. W. *J. Adhes.* **1977**, *8*, 235.
(4) Kim, J.; Han, C. D.; Chu, S. G. *J. Polym. Sci., Part B: Polym. Phys.* **1988**, *26*, 677.
(5) Tse, M. F. *J. Adhes. Sci. Technol*. **1989**, *3*, 551.
(6) Chang, E. P. *J. Adhes*. **1991**, *34*, 189.
(7) Nakajima, N.; Babrowicz, R.; Harrell, E. R. *J. Appl. Polym. Sci.* **1992**, *44*, 1437.
(8) Chang, E. P. *J. Adhes*. **1997**, *60*, 233.
(9) Dahlquist, C. A. Pressure-Sensitive adhesives. In *Treatise on Adhesion and Adhesives*; Patrick, R. L., Ed.; Dekker: New York, 1969; Vol. *2*, p 219.
(10) Zosel, A. *Colloid Polym. Sci*. **1985**, *263*, 541.
(11) Kraus, G.; Rollmann, K. W. *J. Appl. Polym. Sci*. **1977**, *21*, 3311.
(12) Ewins, E. E.; St. Clair, D. J.; Erickson, J. R.; Korcz, W. H. Thermoplastic Rubbers: A-B-A Block Copolymers. In *Handbook of Pressure-Sensitive-Adhesive Technology*, 2nd ed.; Satas, D., Ed.; Van Nostrand Reinhold: New York, 1989; Vol. *1*, p 317.
(13) Lakrout, H.; Sergot, P.; Creton, C. *J. Adhes*. **1999**, *69*, 307.
(14) Shull, K. R.; Creton, C. *J. Polym. Sci., Part B: Polym. Phys*. **2004**, *42*, 4023.
(15) Léger, L.; Creton, C. *Philos. Trans. R. Soc., A* **2008**, *366*, 1425.
(16) Bates, F. S.; Fredrickson, G. H. *Annu. Rev. Phys. Chem*. **1990**, *41*, 525.
(17) Treloar, L. R. G. *Rep. Prog. Phys*. **1973**, *36*, 755.
(18) Gent, A. N. *Rubber Chem. Technol*. **1996**, *69*, 59.
(19) Seitz, M. E.; Martina, D.; Baumberger, T.; Krishnan, V. R.; Hui, C.-Y.; Shull, K. R. *Soft Matter* **2009**, *5*, 447.
(20) Colby, R. H.; Rubinstein, M. *Macromolecules* **1990**, *23*, 2753.
(21) Milner, S. T. *Macromolecules* **2005**, *38*, 4929.
(22) Yu, J. M.; Dubois, P.; Teyssie, P.; Jerome, R. *Macromolecules* **1996**, *29*, 6090.
(23) Weidisch, R.; Michler, G. H.; Arnold, M.; Hofmann, S.; Stamm, M.; Jérôme, R. *Macromolecules* **1997**, *30*, 8078.
(24) Tong, J. D.; Jerome, R. *Macromolecules* **2000**, *33*, 1479.
(25) Tong, J. D.; Jérôme, R. *Polymer* **2000**, *41*, 2499.
(26) Tong, J. D.; Moineau, G.; Leclere, P.; Bredas, J. L.; Lazzaroni, R.; Jerome, R. *Macromolecules* **2000**, *33*, 470.
(27) Tong, J. D.; Leclère, P.; Doneux, C.; Brédas, J. L.; Lazzaroni, R.; Jérôme, R. *Polymer* **2001**, *42*, 3503.
(28) Harrats, C.; Fayt, R.; Jerôme, R. *Polymer* **2002**, *43*, 863.
(29) Tse, M. F.; Jacob, L. *J. Adhes*. **1996**, *56*, 79.
(30) Mori, Y.; Lim, L. S.; Bates, F. S. *Macromolecules* **2003**, *36*, 9879.
(31) Roos, A.; Creton, C. *Macromolecules* **2005**, *38*, 7807.
(32) Daoulas, K.; Theodorou, D. N.; Roos, A.; Creton, C. *Macromolecules* **2004**, *37*, 5093.
(33) Matsen, M. W.; Thompson, R. B. *J. Chem. Phys*. **1999**, *111*, 7139.
(34) Flory, A. L.; Brass, D. A.; Shull, K. R. *J. Polym. Sci., Part B: Polym. Phys. Ed*. **2007**, *45*, 3361.
(35) Mott, P. H.; Roland, C. M.; Hassan, S. E. *Rubber Chem. Technol*. **2003**, *76*, 326.
(36) Seitz, M. E.; Burghardt, W. R.; Faber, K. T.; Shull, K. R. *Macromolecules* **2007**, *40*, 1218.
(37) Drzal, P. L.; Shull, K. R. *J. Adhes*. **2005**, *81*, 397.
(38) Rubinstein, M.; Panyukov, S. *Macromolecules* **2002**, *35*, 6670.
(39) Derail, C.; Cazenave, M. N.; Gibert, F. X.; Marin, G.; Kappes, N.; Lechat, J. *J. Adhes*. **2004**, *80*, 1131.
(40) Gibert, F. X.; Marin, G.; Derail, C.; Allal, A.; Lechat, J. *J. Adhes*. **2003**, *79*, 825.
(41) Roos, A. Ph.D. Thesis, *Sticky Block Copolymers: Structure, Rheological and Adhesive Properties*; Université Paris VI: Paris, 2004; p 350.
(42) Roos, A.; Creton, C. *Macromol. Symp*. **2004**, *214*, 147.
(43) Gibert, F. X. Ph.D. Thesis, Université de Pau et des Pays de l'Adour, Pau, 2001.
(44) Fetters, L. J.; Lohse, D. J.; Colby, R. H. Chain Dimensions and Entanglement Spacings. In *Physical Properties of Polymers Handbook*; Mark, J. E., Ed.; Americal Institute of Physics: New York, 1996; p 335.
(45) Mullins, L.; Tobin, N. *Rubber Chem. Technol*. **1957**, *30*, 555.
(46) Brown, K.; Hooker, J. C.; Creton, C. *Macromol. Mater. Eng*. **2002**, *287*, 163.
(47) Rivals, I.; Personnaz, U.; Creton, C.; Simal, F.; Roose, P.; van Es, S. *Meas. Sci. Technol*. **2005**, *16*, 2020.
(48) Creton, C.; Roos, A.; Chiche, A. Effect of the diblock content on the adhesive and deformation properties of PSAs based on styrenic block copolymers. In *Adhesion: Current Research and Applications*; Possart, W. G., Ed.; Wiley-VCH: Weinheim, 2005; p 337.
(49) Crosby, A. J.; Shull, K. R.; Lakrout, H.; Creton, C. *J. Appl. Phys*. **2000**, *88*, 2956.
(50) Nase, J.; Lindner, A.; Creton, C. *Phys. Rev. Lett*. **2008**, *101*, 074503.
(51) Deplace, F.; Carelli, C.; Mariot, S.; Retsos, H.; Chateauminois, A.; Ouzineb, K.; Creton, C. *J. Adhes*. **2009**, *85*, 18.
(52) Glassmaker, N. J.; Hui, C. Y.; Yamaguchi, T.; Creton, C. *Eur. Phys. J. E* **2008**, *25*, 253.
(53) Krishnan, V. R.; Hui, C. Y. *Eur. Phys. J. E* **2009**, *29*, 61.
(54) Yamaguchi, T.; Doi, M. *Eur. Phys. J. E* **2006**, *21*, 331.
(55) Yamaguchi, T.; Morita, H.; Doi, M. *Eur. Phys. J. E* **2006**, *20*, 7.